

De-Confinement in small systems: Clustering of color sources in high multiplicity $\bar{p}p$ collisions at $\sqrt{s}= 1.8$ TeV

L. G. Gutay^a, A. S. Hirsch^a, C. Pajares^b, R. P. Scharenberg^a, B. K. Srivastava^{a,*}

^a*Department of Physics and Astronomy, Purdue University, West Lafayette, IN-47907, USA*

^b*Departamento de Fisica de Particulas, Universidade de Santiago de Compostela and Instituto Galego de Fisica de Altas Enerxias(IGFAE), 15782 Santiago, de Compostela , Spain*

Abstract

It is shown that de-confinement can be achieved in high multiplicity non jet $\bar{p}p$ collisions at $\sqrt{s}= 1.8$ TeV Fermi National Accelerator Laboratory(FNAL- E735) experiment. Previously the evidence for de-confinement was demonstrated by the constant freeze out energy density in high multiplicity events. In this paper we use the same data but analyze the transverse momentum spectrum in the framework of the clustering of color sources. The charged particle pseudorapidities densities in the range $7.0 \leq \langle dN_c/d\eta \rangle \leq 26.0$ are considered. Results are presented for both thermodynamic and transport properties. The initial temperature and energy density are obtained and compared with the Lattice Quantum Chromo Dynamics(LQCD) simulations. The energy density (ε/T^4) ~ 11.5 for $\langle dN_c/d\eta \rangle \sim 25.0$ is close to the value for 0-10% central events in Au+Au collisions at $\sqrt{s_{NN}}= 200$ GeV. The shear viscosity to entropy density ratio(η/s) is ~ 0.2 at the transition temperature. The result for the trace anomaly Δ is in excellent agreement with LQCD simulations. These results confirm our earlier observation that the de-confined state of matter was created in high multiplicity events in $\bar{p}p$ collisions at $\sqrt{s}=1.8$ TeV.

Keywords: QGP, De-confinement, Shear viscosity, Trace anomaly

1. Introduction

The observation of high total multiplicity, high transverse energy, non-jet, isotropic events led Van Hove [1] and Bjorken [2] to conclude that high energy density events are produced in high energy $\bar{p}p$ collisions [3]. These events have a far greater cross section than the jet production. In these events the transverse energy is proportional to the number of low transverse momentum particles. This basic correspondence can be explored over a wide range of the charged particle pseudorapidity density $\langle dN_c/d\eta \rangle$ in $\bar{p}p$ collisions at center of mass energy $\sqrt{s} = 1.8$ TeV. The analysis of charged particle transverse momentum data from the E735 experiment exhibits flow velocity of mesons and anti-baryons also indicating the possible evidence of QGP formation [4].

Collective hydrodynamics flow has been successful in explaining the AA collisions at RHIC and

LHC energies [5]. However pp collisions have been considered different from the heavy ion collisions. The observation of long range rapidity correlations, the so called “ridge”, similar to that seen in heavy ion collisions in high multiplicity pp collisions at $\sqrt{s}= 7$ TeV by the CMS experiment suggests the evidence of strong radial flow [6, 7]. There are several theoretical papers which support the view that QGP can be formed in high multiplicity pp events [8, 9, 10].

In our earlier work, published in 2002, the evidence of hadronic de-confinement in $\bar{p}p$ collisions at $\sqrt{s} = 1.8$ TeV was presented [11]. Based on the HBT analysis a constant freeze-out energy density $\sim 1 \text{ GeV}/fm^3$ for high multiplicity $\bar{p}p$ events was measured [11]. The freeze-out energy density was found to be independent of the $dN_c/d\eta \geq 6$.

The objective of this work is to further analyze the published E735 data on the transverse momentum spectra of charged particles in the framework of Color String Percolation Model(CSPM). CSPM has been successfully applied to heavy ion

*Corresponding author

Email address: brijesh@purdue.edu (B. K. Srivastava)

data for thermodynamics and transport coefficients [12, 13, 14, 15, 16]. After a brief description of the color string percolation model (CSPM) [17, 18] and the E735 experiment the results are presented for the shear viscosity to entropy density ratio (η/s) and the Equation of State (EOS) of the deconfined matter.

2. String Interactions and Percolation

Multiparticle production at high energies is currently described in terms of color strings stretched between the projectile and target. Hadronizing these strings produce the observed hadrons. The strings act as color sources of particles through the creation of $q\bar{q}$ pairs from the sea. At low energies only valence quarks of nucleons form strings that then hadronize. The number of strings grows with the energy and with the number of nucleons of participating nuclei. Color strings may be viewed as small discs in the transverse space filled with the color field created by colliding partons. Particles are produced by the Schwinger mechanisms [19]. With growing energy and size of the colliding nuclei the number of strings grow and start to overlap to form clusters [17, 18]. At a critical density a macroscopic cluster appears that marks the percolation phase transition. 2D percolation is a non-thermal second order phase transition. In CSPM the Schwinger barrier penetration mechanism for particle production and the fluctuations in the associated string tension due to the strong string interactions make it possible to define a temperature. Consequently the particle spectrum is "born" with a thermal distribution [20]. With an increasing number of strings there is a progression from isolated individual strings to clusters and then to a large cluster which suddenly spans the area. In two dimensional percolation theory the relevant quantity is the dimensionless percolation density parameter given by [17, 18]

$$\xi = \frac{NS_1}{S_\perp} \quad (1)$$

where N is the number of strings formed in the collisions and S_1 is the transverse area of a single string and S_\perp is the transverse nuclear overlap area. The critical cluster which spans S_\perp , appears for $\xi_c \geq 1.2$ [21, 22]. As ξ increases the fraction of S_\perp covered by this spanning cluster increases.

We assume that a cluster of n strings behaves as a single string with an energy-momentum that

corresponds to the sum of energy-momenta of the individual strings and with a higher color field, corresponding to the vectorial sum of the color field of each individual string [17, 18]. One can obtain the multiplicity μ and the mean transverse momentum squared $\langle p_t^2 \rangle$ of the particles produced by a cluster of n strings [18]

$$\mu_n = \sqrt{\frac{nS_n}{S_1}} \mu_0; \quad \langle p_t^2 \rangle = \sqrt{\frac{nS_1}{S_n}} \langle p_t^2 \rangle_1 \quad (2)$$

where μ_0 and $\langle p_t^2 \rangle_1$ are the mean multiplicity and $\langle p_t^2 \rangle$ of particles produced from a single string with a transverse area $S_1 = \pi r_0^2$. In the limit of high string density, one obtains [17, 18]

$$\langle \frac{nS_1}{S_n} \rangle = \frac{\xi}{1 - e^{-\xi}} \equiv \frac{1}{F(\xi)^2} \quad (3)$$

where $F(\xi)$ is the color suppression factor. $F(\xi)$ is related to the ξ .

$$F(\xi) = \sqrt{\frac{1 - e^{-\xi}}{\xi}}. \quad (4)$$

The net effect due to $F(\xi)$ is the reduction in hadron multiplicity and increase in the average transverse momentum of particles. The CSPM model calculation for hadron multiplicities and momentum spectra were found to be in excellent agreement with experiment [15].

It is worth noting that CSPM is a saturation model similar to the Color Glass Condensate (CGC), where $\langle p_t^2 \rangle_1 / F(\xi)$ plays the same role as the saturation momentum scale Q_s^2 in the CGC model [23, 24].

3. E735 experiment

Experiment E735 was run during the 1988-1989 Tevatron running period, primarily collecting data triggered to enrich high multiplicity events in \bar{p} collisions at $\sqrt{s} = 1.8$ TeV [25]. The E735 was located at the C_ϕ interaction region of the Fermi National Accelerator Laboratory (FNAL) [25, 26, 27]. The $\bar{p}p$ interaction region was surrounded by a cylindrical drift chamber which in turn was covered by a single layer hodoscope including endcaps. This system measured the total charged particle multiplicity $10 < N_c < 200$ in the pseudorapidity range $|\eta| < 3.25$. A sidearm magnetic spectrometer with tracking chambers and time of flight counters, provided particle identified momenta spectra in the

range $0.1 < p_t < 1.5$ GeV/c. The spectrometer covered $0.37 < \eta < +1.00$ with $\Delta\phi \sim 20^\circ$ (ϕ is the azimuthal angle around the beam direction).

The multiplicity dependence of the transverse momentum p_t spectra was measured in $\bar{p}p$ collisions at $\sqrt{s} = 1.8$ TeV [27]. The invariant p_t spectra was fitted with a power law $A/(p_0 + p_t)^n$ [28]. Table 1 shows the power law fit parameters for high multiplicity events [27].

Table 1: Number of tracks N_c as measured by the E735 experiment in the pseudorapidity range $|\eta| < 3.25$, $\langle dN_c/d\eta \rangle$, and the fit parameters p_0 and n to the invariant p_t distribution [26, 27].

N_c	$\langle dN_c/d\eta \rangle$	p_0	n
47 (minbias)	7.3	1.25	8.35
85	13.07	1.052	7.038
105	16.15	1.001	6.743
135	20.76	1.001	6.581
165	25.38	1.061	6.766

4. Determination of the color suppression factor $F(\xi)$

The suppression factor is determined by comparing the charged particle spectra from low energy pp collisions and high multiplicity transverse momentum spectra from $\bar{p}p$. To evaluate the initial value of ξ from data a parameterization of pp events at $\sqrt{s} = 200$ GeV is also used to compute the p_t distribution

$$dN_c/dp_t^2 = a/(p_0 + p_t)^n \quad (5)$$

where a is the normalization factor. $p_0 = 1.98$ and $n = 12.88$ are parameters used to fit the data. This parameterization is used for high multiplicity events in $\bar{p}p$ collisions at $\sqrt{s} = 1.8$ TeV to take into account the interactions of the strings [18].

$$dN_c/dp_t^2 = \frac{a'}{(p_0 \sqrt{F(\xi_{pp})/F(\xi_{\bar{p}p})} + p_t)^n} \quad (6)$$

In pp collisions $F(\xi_{pp}) \sim 1$ at $\sqrt{s} = 200$ GeV due to the low overlap probability [12]. Figure (1) shows a plot of $F(\xi)$ as a function of charged particle multiplicity per unit transverse area $\frac{dN_c}{d\eta}/S_\perp$ for high multiplicity events along with the minbias events. For pp collisions the overlap area S_\perp is taken as the inelastic pp cross section σ_{pp} [29, 30, 31]. For

$\bar{p}p$ collision at $\sqrt{s}=1.8$ $\sigma_{\bar{p}p} \sim 60$ mb [30]. The error on $F(\xi)$ is $\sim 6\%$. The transverse overlap area measured in E735 by Hanbury-Brown-Twiss is in excellent agreement with this inelastic cross section [11]. The results from Au+Au collisions at $\sqrt{s_{NN}} = 200$ GeV [14, 16] are also shown in Fig. (1).

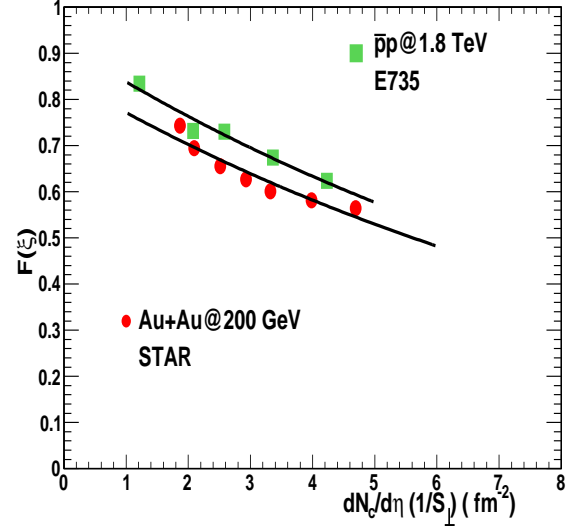


Figure 1: The color suppression factor $F(\xi)$ as a function of $\frac{dN_c}{d\eta}/S_\perp$ (fm^{-2}). The solid green squares are from $\bar{p}p$ at $\sqrt{s}=1.8$ TeV. The solid red circles are for Au+Au collisions at $\sqrt{s_{NN}} = 200$ GeV (STAR data) [14]. The error is smaller than the size of the symbol. Lines are fit to $\bar{p}p$ and the STAR data.

5. Temperature

The connection between the measured $F(\xi)$ and the temperature $T(\xi)$ involves the Schwinger mechanism (SM) for particle production. The Schwinger distribution for massless particles is expressed in terms of p_t^2 [19, 32]

$$dn/dp_t^2 \sim e^{-\pi p_t^2/x^2} \quad (7)$$

where the average value of the string tension is $\langle x^2 \rangle$. The tension of the macroscopic cluster fluctuates around its mean value because the chromo-electric field is not constant. The origin of the color string fluctuation is related to the stochastic picture of the QCD vacuum. Since the average value of the color field strength must vanish, it can not be constant but changes randomly from point to point

Table 2: $\langle dN_c/d\eta \rangle$, the measured percolation density parameter ξ , initial temperature T , initial energy density ε and η/s for $\bar{p}p$ $\sqrt{s}=1.8$ TeV

$\langle dN_c/d\eta \rangle$	ξ	T (MeV)	$\varepsilon(GeV/fm^3)$	η/s
7.30(minbias)	0.778	160.31	0.50	0.30
13.07	1.39	170.73	0.86	0.23
16.15	1.42	171.22	1.07	0.23
20.76	1.84	178.06	1.39	0.21
25.38	2.30	185.07	1.75	0.21

[20]. Such fluctuations lead to a Gaussian distribution of the string tension for the cluster, which gives rise to the thermal distribution [12, 20, 33]

$$dn/dp_t^2 \sim e^{(-p_t \sqrt{\frac{2\pi}{\langle x^2 \rangle}})} \quad (8)$$

with $\langle x^2 \rangle = \pi \langle p_t^2 \rangle_1 / F(\xi)$. The temperature is expressed as

$$T(\xi) = \sqrt{\frac{\langle p_t^2 \rangle_1}{2F(\xi)}} \quad (9)$$

where $\langle p_t^2 \rangle_1$ is the average transverse momentum squared of particles produced from a single string. At the percolation transition $\xi = 1.2$ and the critical value of the temperature is taken $T_c = 167$ MeV from the statistical model, which is the universal chemical freeze-out temperature and is a good measure of the phase transition temperature [34, 35]. This determines $\sqrt{\langle p_t^2 \rangle_1} = 207$ MeV [12]. The temperature obtained using Eq. (9) for $\langle dN_c/d\eta \rangle \sim 25$ is ~ 188 MeV. This temperature is closed to ~ 193.6 MeV obtained for 0-10 %Au+Au collisions at $\sqrt{s_{NN}} = 200$ GeV [12].

6. Energy Density

Among the most important and fundamental problems in finite-temperature QCD are the calculation of the bulk properties of hot QCD matter and characterization of the nature of the QCD phase transition. The QGP according to CSPM is born in local thermal equilibrium because the temperature is determined at the string level. After the initial temperature $T > T_c$ the CSPM perfect fluid may expand according to Bjorken boost invariant 1D hydrodynamics [36]

$$\varepsilon = \frac{3}{2} \frac{\frac{dN_c}{dy} \langle m_t \rangle}{S_\perp \tau_{pro}} \quad (10)$$

where ε is the energy density, S_\perp the transverse overlap area of the colliding nuclei, and τ_{pro} the proper time. Above the critical temperature only massless particles are present in CSPM. To evaluate ε we use the charged pion multiplicity dN_c/dy . The factor 3/2 in Eq.(12) accounts for the neutral pions. The average transverse mass $\langle m_t \rangle$ is given by $\langle m_t \rangle = \sqrt{\langle p_t \rangle^2 + m_0^2}$, where $\langle p_t \rangle$ is the average transverse momentum of pion and m_0 the mass of pion. In Schwinger model τ_{pro} is given by $\tau_{pro} = \frac{2.405\hbar}{\langle m_t \rangle}$ [19].

The pion multiplicity was obtained from the total multiplicity after subtracting the contributions due to kaons and protons [25, 37]. The average p_t $\langle p_t \rangle$ for pions are flat in the region $7 \leq \langle dN_c/d\eta \rangle \leq 26$. Table 2 shows the values of ε and temperature for various values of $\langle dN_c/d\eta \rangle$. With the determina-

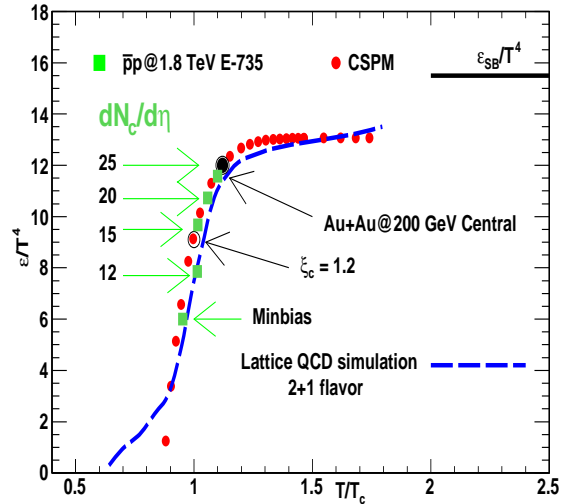


Figure 2: ε/T^4 as a function of T/T_c . Solid green squares are from $\bar{p}p$ collisions at $\sqrt{s} = 1.8$ TeV. The lattice QCD calculation is shown as dotted blue line [38]. CSPM for Au+Au at $\sqrt{s_{NN}} = 200$ GeV are red solid circles [14].

tion of T and ε one can compare the energy density expressed as ε/T^4 with the available lattice QCD results [38]. Figure 2 shows a plot of ε/T^4 as a function of T/T_c . The lattice QCD results are from the HotQCD Collaboration [38]. The result for most central collisions for Au+Au at $\sqrt{s_{NN}} = 200$ GeV is also shown in Fig.2. It is observed that for highest multiplicity $\langle dN_c/d\eta \rangle \sim 27$, ε/T^4 is close to the value obtained for Au+Au at 200 GeV. The minimum bias result is below the percolation threshold. This result confirms the formation of the QGP in

high multiplicity events in $\bar{p}p$ interactions at $\sqrt{s} = 1.8$ TeV.

7. Shear viscosity to entropy density ratio η/s

In our earlier work the shear viscosity to entropy density ratio η/s was obtained in the framework of kinetic theory and the string percolation [14]. The following expression was obtained for η/s [39, 40, 14].

$$\frac{\eta}{s} = \frac{TL}{5(1 - e^{-\xi})} \quad (11)$$

where T is the temperature and L is the longitudinal extension of the source ~ 1 fm.

Fig. 3 shows η/s as a function of the temperature [14]. The lower bound shown in Fig. 3 is given by the AdS/CFT conjecture [41].

The results from Au+Au at $\sqrt{s_{NN}} = 200$ GeV collisions are also shown in Fig. 3 for comparison purposes. It is seen that for $\langle dN_c/d\eta \rangle \sim 25$ the η/s is equal to the value from the most central collisions in Au+Au at 200 GeV.

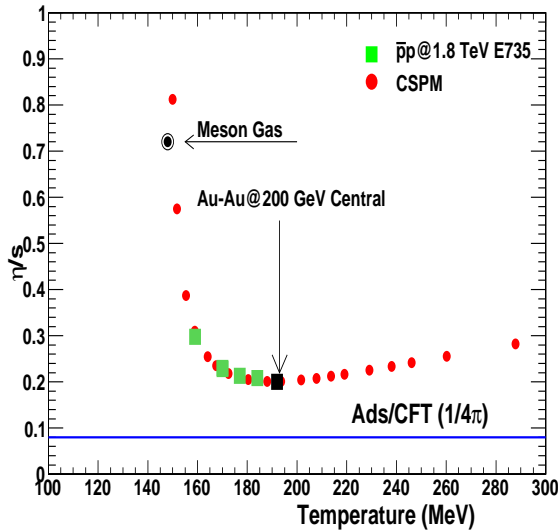


Figure 3: η/s as a function of temperature T using Eq. (11) [14]. Solid green squares are from $\bar{p}p$ collisions at $\sqrt{s} = 1.8$ TeV. CSPM results for Au+Au at $\sqrt{s_{NN}} = 200$ GeV are shown as solid red circles [14]. The meson gas value for $\eta/s \sim 0.7$ is shown as solid black circle at $T \sim 150$ MeV [42]. The lower bound shown is given by the AdS/CFT [41].

8. η/s and Trace anomaly Δ

The trace anomaly (Δ) is the expectation value of the trace of the energy-momentum tensor, $\langle \Theta^\mu_\mu \rangle = (\varepsilon - 3p)$, which measures the deviation from conformal behavior and thus identifies the interaction still present in the medium [43]. We find that the reciprocal of η/s is in quantitative agreement with $(\varepsilon - 3p)/T^4$ from LQCD over a wide range of temperatures [13, 15]. Fig. 4 shows the Δ for $\bar{p}p$ along with the CSPM calculation and LQCD simulations. The minimum in $\eta/s \sim 0.20$ determines the peak of the interaction measure ~ 5 in agreement with the recent HotQCD values [44]. Figure 4 also shows the results from the Wuppertal Collaboration [45]. The maximum in Δ corresponds to the minimum in η/s . This is true for the highest multiplicity events in $\bar{p}p$ collisions.

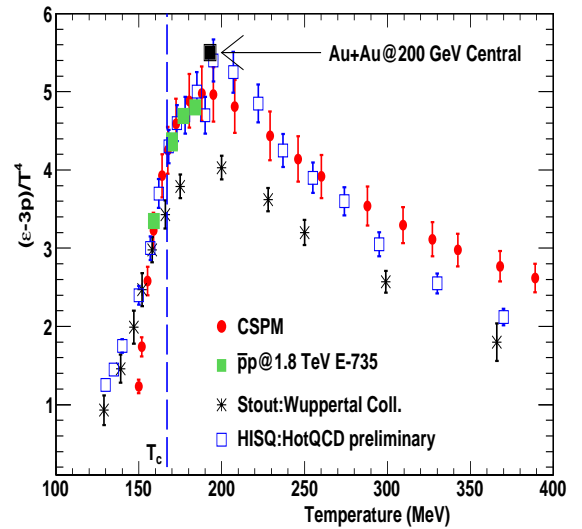


Figure 4: The trace anomaly $\Delta = (\varepsilon - 3p)/T^4$ vs temperature [44]. Solid green squares are from $\bar{p}p$ collisions at $\sqrt{s} = 1.8$ TeV. Blue open squares are from HotQCD Collaboration [44]. Black stars are from Wuppertal Collaboration [45].

9. Equation of State: Sound velocity

We use CSPM coupled to a 1D Bjorken expansion. The input parameters are the initial temperature T , the initial energy density ε , and the trace anomaly Δ are determined by data. The Bjorken 1D expansion for the sound velocity can be written [36]

$$\frac{dT}{d\varepsilon} s = C_s^2. \quad (12)$$

In the above equation the entropy density s is expressed as $s = (\varepsilon + P)/T$. The pressure P is related to trace anomaly $P = (\varepsilon - \Delta T^4)/3$. We can express C_s^2 in terms of ξ

$$C_s^2 = (-0.33) \left(\frac{\xi e^{-\xi}}{1 - e^{-\xi}} - 1 \right) + 0.0191(\Delta/3) \left(\frac{\xi e^{-\xi}}{(1 - e^{-\xi})^2} - \frac{1}{1 - e^{-\xi}} \right) \quad (13)$$

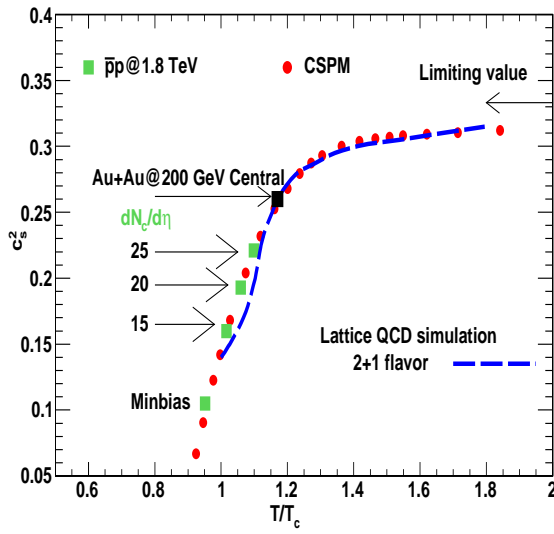


Figure 5: The speed of sound from CSPM (red circles) and Lattice QCD-p4 (blue dash line) versus T/T_c [38]. The green solid squares are from $\bar{p}p$ at $\sqrt{s} = 1.8$ TeV.

Since there is no direct way to obtain pressure in CSPM, we have made the assumption that the dimensionless ratio $\Delta = (\varepsilon - 3P)/T^4 \approx 1/(\eta/s)$. Fig. 5 shows a plot of C_s^2 as a function of T/T_c . It is observed that the CSPM results are in very good agreement with the lattice calculations [38]. This suggests that the Δ as obtained from the data can be represented by $1/(\eta/s)$.

10. Summary

The $\bar{p}p$ collisions at $\sqrt{s} = 1.8$ TeV from the E735 experiment have been analyzed in using the clustering of color sources phenomenology. The results for temperature, energy density and transport coefficient have been extracted for high multiplicity events. The trace anomaly is also obtained and compared with the LQCD results. The clustering

of color sources has shown that the determination of η/s as a function of temperature is an important quantity that relates to the trace anomaly Δ . The main assumption of the present approach is that the inverse of η/s represents the trace anomaly, $\Delta = (\varepsilon - 3p)/T^4$. The clustering of color sources (percolation) provides us with a microscopic partonic picture that also connects the transport properties of the QGP to its thermodynamics.

These results strongly suggest that even in small systems at high energy and high multiplicity events QGP formation is possible as seen in $\bar{p}p$ collisions at $\sqrt{s} = 1.8$ TeV.

The analysis of the pp collisions at $\sqrt{s} = 7$ and 14 TeV at the CERN LHC can map event higher temperatures and energy densities. Then it will be possible to obtain the trace anomaly at higher temperature as shown in Fig.(4). The attenuation of high p_t particles in high multiplicity events would be a second signal that the de-confined matter is indeed the QGP.

11. Acknowledgment

This research was supported by the Office of Nuclear Physics within the U.S. Department of Energy Office of Science under Grant No. DE-FG02-88ER40412. CP thanks Ministry of Economy of Spain and FEDER funds for financial support.

References

- [1] L. V. Hove, Phys. Lett. B 118 (1982) 138.
- [2] J. D. Bjorken, Fermilab Pub. 82/44-THY.
- [3] L. McLerran, Rev. Mod. Phys. 58 (1986) 1021.
- [4] P. Levai, B. Muller, Phys. Rev. Lett. 67 (1991) 1519.
- [5] U. Heinz, R. Snellings, Ann. Rev. Nucl. Part. Sci 63 (2013) 123.
- [6] V. Khachatryan et al. (CMS Collaboration), JHEP 1009 (2010) 091.
- [7] T. Kalaydzhyan, E. Shuryak, arXiv:1503.0521.
- [8] K. Werner, B. Guiot, I. Karpenko, T. Piergo, Nucl. Phys. A 931 (2014) 83.
- [9] C. Andres, A. Moscoso, C. Pajares, Phys. Rev. C 90 (2014) 054902.
- [10] P. Ghosh, S. Muhuri, J. K. Nayak, R. Varma, J. Phys. G 41 (2014) 03516.
- [11] T. Alexopoulos et al. (E735 Collaboration), Phys. Lett. B 528 (2002) 43.
- [12] R. P. Scharenberg, B. K. Srivastava, A. S. Hirsch, Eur. Phys. J. C 71 (2011) 1510.
- [13] R. P. Scharenberg, PoS (CPOD 2013) 017.
- [14] J. D. de Deus, A. S. Hirsch, C. Pajares, R. P. Scharenberg, B. K. Srivastava, Eur. Phys. J. C 72 (2012) 2123.
- [15] B. K. Srivastava, Nucl. Phys. A 926 (2014) 142.
- [16] M. A. Braun, J. D. de Deus, A. S. Hirsch, C. Pajares, R. P. Scharenberg, B. K. Srivastava, arXiv:1501.01524.

- [17] M. A. Braun, C. Pajares, Eur. Phys. J. C 16 (2000) 349.
- [18] M. A. Braun, F. del Moral, C. Pajares, Phys. Rev. C 65 (2002) 024907.
- [19] J. Schwinger, Phys. Rev. 128 (1962) 2425.
- [20] A. Bialas, Phys. Lett. B 466 (1999) 301.
- [21] M. B. Isichenko, Rev. Mod. Phys. 64 (1992) 961.
- [22] H. Satz, Rep. Prog. Phys. 63 (2000) 1511.
- [23] L. McLerran, R. Venugopalan, Phys. Rev. D 49 (1994) 2233.
- [24] J. D. de Deus, C. Pajares, Phys. Lett. B 695 (2011) 211.
- [25] T. Alexopoulos et al. (E735 Collaboration), Phys. Rev. D 48 (1993) 984.
- [26] T. Alexopoulos et al. (E735 Collaboration), Phys. Lett. B 336 (1994) 599.
- [27] T. Alexopoulos et al. (E735 Collaboration), Phys. Lett. B 435 (1998) 453.
- [28] C. Albajar et al. (UA1 Collaboration), Nucl. Phys. B 335 (1990) 261.
- [29] B. I. Abelev et al. (STAR Collaboration), Phys. Rev. C 79 (2009) 34909.
- [30] S. Klimenko, J. Konigsberg, T. M. Liss, Fermilab-FN-0741(2003).
- [31] B. Abelev et al. (ALICE Collaboration), Eur. Phys. J. C 73 (2013) 2456.
- [32] C. Y. Wong, Introduction to high energy heavy ion collisions, 1994.
- [33] J. D. de Deus, C. Pajares, Phys. Lett. 642 (2006) 455.
- [34] P. Braun-Munzinger, J. Stachel, C. Wetterich, Phys. Lett. B 596 (2004) 61.
- [35] F. Becattini, P. Castorina, A. Milov, H. Satz, Eur. Phys. J. C 66 (2010) 377.
- [36] J. D. Bjorken, Phys. Rev. D 27 (1983) 140.
- [37] T. Alexopoulos et al. (E735 Collaboration), Phys. Rev. Lett. 64 (1990) 991.
- [38] A. Bazavov et al., Phys. Rev. D 80 (2009) 014504.
- [39] P. Danielewicz, M. Gyulassy, Phys. Rev. D 31 (1985) 53.
- [40] T. Hirano, M. Gyulassy, Nucl. Phys. A 769 (2006) 71.
- [41] P. K. Kovtun, D. T. Son, A. O. Starinets, Phys. Rev. Lett. 94 (2005) 111601.
- [42] M. Prakash, M. Prakash, R. Venugopalan, G. Wleke, Phys. Rep. 227 (1993) 321.
- [43] M. Cheng et al., Phys. Rev. D 80 (2010) 054504.
- [44] P. Petreczky, Lattice 2012 Cairns, Australia (24 - 30 June).
- [45] S. Borsanyi et al., Phys. Rev. D 80 (2009) 014504.